Optical properties of the two-port resonant tunneling filters in two-dimensional photonic crystal slabs*

Ren Cheng(任 承)[a)†], Cheng Li-Feng(程立锋)[a)], Kang Feng(康 凤)[b)], Gan Lin(甘 霖)[c)], Zhang Dao-Zhong(张道中)[c)], and Li Zhi-Yuan(李志远)[c)]

[a)] *School of Opto-Electronic Information Science and Technology, Yantai University, Yantai* 264005, *China*

[b)] *Wenjing College, Yantai University, Yantai* 264005, *China*

[c)] *Optical Physics Laboratory, Institute of Physics, Chinese Academy of Sciences, Beijing* 100190, *China*

(Received 29 June 2012; revised manuscript received 10 July 2012)

We have designed and fabricated two types of two-port resonant tunneling filters with a triangular air-hole lattice in two-dimensional photonic crystal slabs. In order to improve the filtering efficiency, a feedback method is introduced by closing the waveguide. It is found that the relative position between the closed waveguide boundary and the resonator has an important impact on the dropping efficiency. Based on our analyses, two different types of filters are designed. The transmission spectra and scattering-light far-field patterns are measured, which agree well with theoretical prediction. In addition, the resonant filters are highly sensitive to the size of the resonant cavities, which are useful for practical applications.

Keywords: photonic crystal slabs, filter, finite-difference time-domain method

PACS: 42.70.Qs, 42.82.Gw, 42.25.Bs **DOI:** 10.1088/1674-1056/21/10/104210

1. Introduction

Photonic crystals (PCs)[1,2] have become the focus of much attention because photonic band gap (PBG) can be realized by these materials with periodically modulated refraction index. Many studies have shown that two-dimensional (2D) PC slabs with high index contrast possess many advantages, such as large in-plane PBGs and ease to be fabricated compared with their three-dimensional (3D) counterparts. In 2D PC slabs, light waves are confined by a combination of the in-plane PBG confinement and vertical total-internal-reflection (TIR) confinement. Various photonic devices can be realized by introducing artificial defects in 2D PC slabs, such as waveguides,[3−8] microcavities,[9,10] and filters.[11−21]

Optical filters are the essential components for photonic integrated circuits and dense wavelength-division-multiplexing (WDM) optical communication systems. Particularly, simple resonant tunneling filter can function as an effective device of wavelength filtering for the extraction of light trapped in a point-defect cavity to another neighboring waveguide. However, when mentioning the practical applications of the filter devices in 2D PC slabs, much attention should be paid to some key problems. First, the resonant filters should have high coupling efficiency between cavities and input/output waveguides in practical 2D PC slabs. In Ref. [11], the dropping efficiency of the simplest resonant tunneling filter is only 25% in theory because the light is output from the four ends of the two waveguides, which is not suitable for practical applications. Therefore, different designs have been proposed to solve the problem. For example, Noda *et al.*[12−15] demonstrated that the dropping efficiency can be improved greatly by the reflection feedback of the heterostructure interfaces. However, the bent waveguides have to be introduced, and optimization of the distance between a resonator and a hetero interface is required. Moreover, the resonant filters should feel the subtle changing of the resonant frequency when finely tuning the size of the resonant cavities at present micro-fabrication precision.

In this paper, we present two types of two-port resonant tunneling filters with a size on the order of ten micrometers in 2D PC slabs by closing the bus waveguide for reflection feedback. Because of the dis-

*Project supported by the National Natural Science Foundation of China (Grant No. 11004169), the National Basic Research Program of China (Grant No. 2011CB922002), and the Doctoral Foundation of Shandong Province, China (Grant No. BS2009CL028).

†Corresponding author. E-mail: cren@ytu.edu.cn

© 2012 Chinese Physical Society and IOP Publishing Ltd

tinct impact of the relative position on the dropping efficiency, different designs are introduced and their optical properties are measured, respectively. The results are conducive to design high-performance photonic devices. In our design, bent waveguides are abstained, and careful consideration of interference process is not required, which leads to a high dropping efficiency. In addition, the designed filter is highly sensitive to the size of the resonant cavities fabricated at present micro-fabrication precision. All facts imply that this filter may be a good candidate for wavelength filtering and other optical operations in ultra-compact photonic integrated circuits.

2. Design and analysis

Our two-port resonant tunneling filter consists of one input waveguide, one output waveguide, and a resonant cavity between them. In order to improve the dropping efficiency, we introduce two perfect reflection mirrors at the input and output waveguides by closing both waveguides. According to the coupled-mode analysis,[21] the relative position between the closing waveguide boundary and the resonator has an impact on the dropping efficiency. However, there is no experimental evidence yet. Moreover, what transformation on the transmission spectra will occur when changing the position of the closing waveguide boundary is uncertain, which is imperative for the practical application of the filter. Therefore, we design different types of filters, where the lengths of the bus waveguides are slightly different.

The schematic diagram of type-I filter is shown in Fig. 1(a). P1 and P2 are the input and output waveguides, respectively, which are formed by filling one row of air holes along the Γ–K direction of PC built on an air-bridged silicon slab, and symmetrically arranged with respect to the center of resonator C1. The lattice constant of the PC and the hole diameter are 420 nm and 270 nm, respectively. C1 is a three-point-defect cavity, so-called L3 cavity. As is known, the slight shift of air holes is conducive to confine light inside the cavity and leads to a high quality factor. The two air holes at the defect-cavity edges are shifted outward by $0.25a$ from the regular positions, where a is the lattice constant of the PC. The distance from the closing waveguide boundary to the center of the resonator in the x direction is $-4a$. The distance between the centers of the defect cavities and the neighboring waveguide is three rows of holes in the y direction.

The 3D finite-difference time-domain (FDTD) method is used to calculate the resonant frequencies of C1 with TE-like polarization. The calculated resonant wavelength of C1 is about 1521.1 nm. The refractive index of silicon is 3.4, and the thickness of the silicon slab is about 235 nm. Other parameters take the same values as the design. Figure 1(b) shows the distribution of magnetic field H_z in the central plane of the silicon slab, which has even symmetry with respect to the mirror refection plane passing through the waveguide central axis. It clearly shows that the resonant mode of resonator C1 expands in four directions, and the light tunnels into the P1 boundary and reaches P2 when the frequency is resonant. Interference occurs between the light coupled out from the resonator and that reflected back from the waveguide boundary, which may destructively disturb the shape of the transmission spectra.

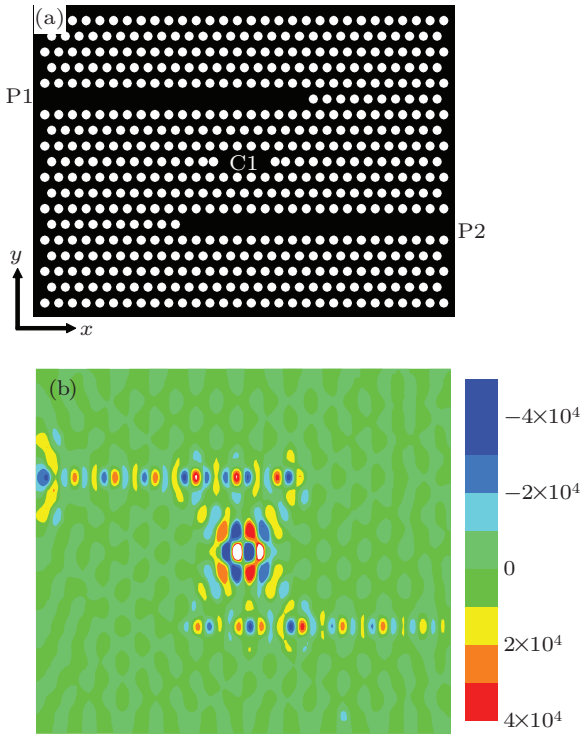


Fig. 1. (colour online) (a) Schematic diagram of the two-port resonant tunneling filter (type I). (b) Magnetic field profile (H_z) when the frequency is on-resonant.

Type-II filter, as shown schematically in Fig. 2(a), has the similar structure as type-I filter except a bit shorter length of waveguides P1 and P2. The distance between the waveguide boundary and the center of the resonator in the x direction is $4a$. The same resonant cavity C1 is used. The magnetic field (H_z) profiles are shown in Fig. 2(b) when C1 is on-resonance. For

type-II filter, the coupling regions are on the waveguide boundary. The phases of the light coupled out from the resonator and the light reflected back from the waveguide boundary are always opposite, and the output toward P1 is automatically eliminated. Accordingly, most of energy is localized in the resonator C1, as shown in Fig. 2(b), which indicates a high quality factor in this case. When the frequency is off-resonant, strong reflection occurs at the P1 boundary.

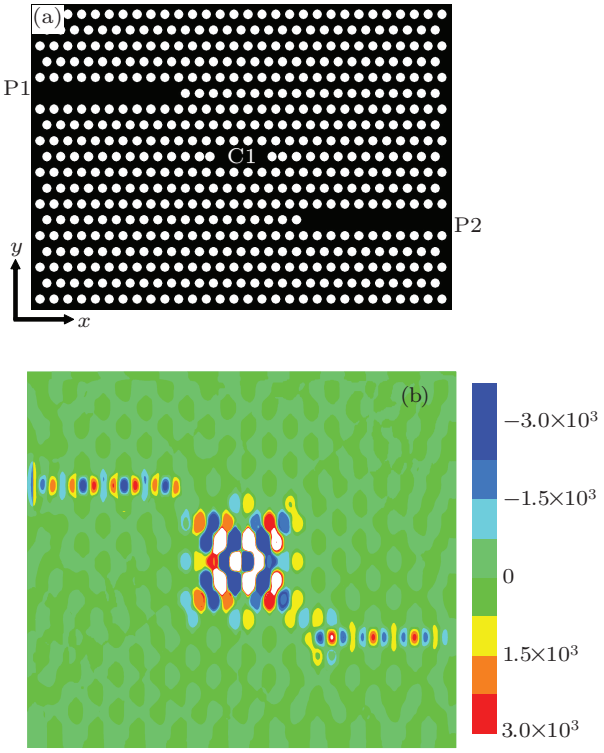


Fig. 2. (colour online) (a) Schematic diagram of the two-port resonant tunneling filter (type II). (b) Magnetic field profile (H_z) when the frequency is on-resonant.

3. Fabrication and optical properties

The designed samples are fabricated on a silicon-on-insulator (SOI) wafer by a combination of electron beam lithography (Raith 150, Germany) and inductively coupled plasma dry etching under the atmosphere of SF_6 and C_4F_8 gases. Finally, the insulator layer beneath the PC area is removed by hydrogen fluoride (HF) acid to form an air-bridged structure. The top silicon layer of the SOI wafer is about 235 nm.

Figure 3(a) shows the scanning electron micrograph (SEM) of the fabricated sample of type-I filter. The lattice constant of the PC and the radius of the air holes are the same as that used in the FDTD simulation. The filter consists of one input waveguide (P1) and one output waveguide (P2). The C1 is the as-designed cavity generated by neglecting three air holes. The light source is a tunable CW laser ranging from 1500 nm to 1640 nm with the maximum power of about 10 mW. The laser is coupled into P1 via a single-mode lensed fiber, and the output light is collected by a highly sensitive InGaAs detector via another single-mode lensed fiber. The intensity of vertically scattered light is monitored with an infrared camera. In order to investigate the dropping performance, the transmission spectra are measured at outlet P2. The result is shown in Fig. 3(b). The transmission peak is located between 1520 nm and 1540 nm. Moreover, multiple oscillating peaks appear at the top. According to the magnetic field (H_z) profiles (see Fig. 1(b)), we know that the oscillating peaks on the top may be caused by the destructive interference between the light coupled out from the resonator and that reflected back from the waveguide boundary.

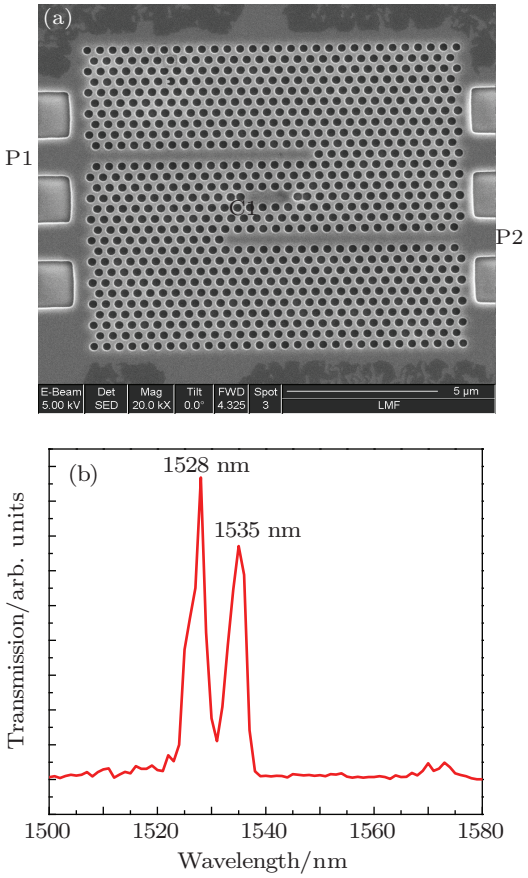


Fig. 3. (colour online) (a) SEM image of the fabricated sample of type-I filter. (b) The measured transmission spectra at P2.

Figure 4(a) shows the SEM image of the fabricated sample of type-II filter, which has the same parameters as design. In order to compare the dropping

performance with that of type-I filter, the transmission spectra are measured at the output waveguide P2. Figure 4(b) shows the measured result. A single sharp peak appears at 1539 nm within the wavelength range of 1500 nm–1580 nm, and its full width at half maximum is only 3 nm. The results indicate that in-plane filtering has been successfully achieved at a broader bandwidth of 80 nm. It is obviously found that type-II filter has a better filtering performance than type-I filter by comparing Fig. 3(b) with Fig. 4(b). The above result proves that the relative distance between the closed waveguide and resonator plays an important role in determining the mode matching among waveguides, resonator, and the corresponding filtering performance. To estimate the dropping efficiency, a reference straight waveguide of the same parameters is located near the two-port resonant tunneling filter. By maintaining the intensity of input light and keeping the input light at 1539 nm, the transmission intensities of the reference waveguide and P2 are fixed at 0.3 μW and 0.12 μW, respectively. The dropping efficiency is estimated to be 40%.

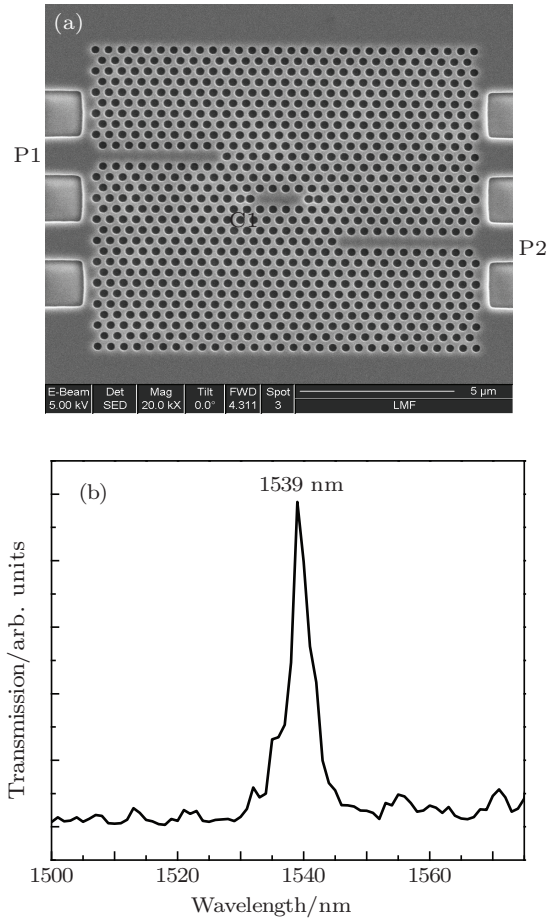


Fig. 4. (a) SEM image of the fabricated sample of type-II filter. (b) The measured transmission spectra at P2.

In order to observe the light propagation directly in the two filters, we measured the far-field pattern (FFP) by using an infrared camera set on the top of the sample. This far-field intensity corresponds to the scattering of optical near field by roughness in the silicon structure, and is well proportional to the near field intensity. Therefore, it can roughly probe the near-field pattern of optical wave transporting in the silicon PC structure. Figures 5(a) and 5(b) show the FFPs of type-I and type-II filters when they are on-resonant, respectively. As shown in Fig. 5(a), when type-I filter is on the resonant state, the input light is trapped and then emitted from cavity C1. Moreover, another bright spot appears at the neighboring lower position of cavity C1, which may be caused by the strong interference between the light coupled out from the resonator C1 and that reflected back from the waveguide P2 boundary. Correspondingly, one bright spot will appear at the output end of P2. Comparatively, when type-II filter is on the resonant state (see Fig. 5(b)), stronger scattering light is observed at the cavity C1 than that of type-I filter. However, the bright spot at the neighboring lower position of cavity C1 disappears, which means that the destructive interference existing in type-I filter is removed. Simultaneously, behaviors similar to that of type-I filter can be observed at the output end P2. The FFPs agree well with the theoretical simulation shown in Figs. 1(b) and 2(b). The results show that this scattering-light analysis technique can be a helpful complementary tool for the quantitative transmission spectrum measurement.

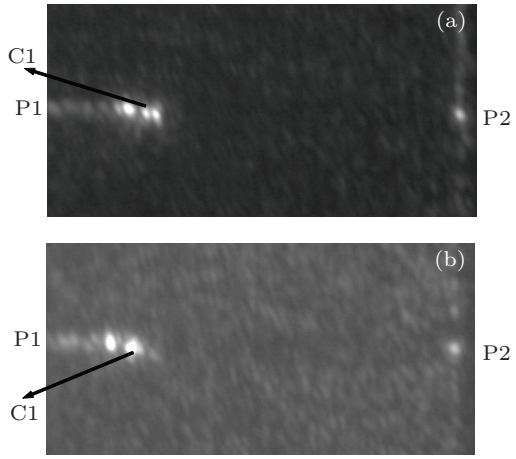


Fig. 5. Far-field images when the frequency is on-resonant for (a) type-I filter and (b) type-II filter.

In the above discussions, the resonator C1 is a three-point defect cavity, which is formed by shifting two air holes at the defect-cavity edges outward by $0.25a$ relative to the regular positions. For

practical applications, it is important that the resonant filter can feel the subtle change in the resonant frequency when finely shifting the size of the resonant cavity, which means a highly sensitive photonic device. For this purpose, we move the end air holes at defect-cavity edges outward by $0.2a$, $0.1a$, and $0.05a$, and designate them as resonators C2, C3, and C4, respectively. If the above resonators are used in the designed resonant filter of type-II filter, different filter properties can be achieved in theory. The calculated resonant wavelengths of C2, C3, and C4 are about 1519.5, 1517.3, and 1514.0 nm, respectively. The related parameters take the same values as that of the designed type-II filter. Now we want to know whether the real samples fabricated at present micro-fabrication precision can feel the subtle change in resonant cavities. For this purpose, we fabricate the samples and measure the transmission spectra at their own output waveguides. Figure 6 shows the measured results by tuning the wavelength of incident light. Three single sharp resonant peaks corresponding to C2, C3, and C4 in type-II filter appear within the wavelength range of 1500 nm–1680 nm, which indicates that tunable in-plane filtering has been successfully achieved. For a broader band width of 80 nm, single mode operation is possible, which is a favorable feature for practical applications, e.g., the wave division multiplexer. The resonant wavelengths of C2, C3, and C4 are 1538, 1537, and 1535 nm, corresponding to Figs. 6(a), 6(b), and 6(c), respectively. In spite of slight shift in the measured resonant peak toward lower frequency, the experimental results are in fairly good agreement with the simulation results. Particularly, the measured wavelength spacing between adjacent cavities C1, C2, C3, and C4 are 1, 1, and 2 nm, which agree well with the theoretical simulation results (1.6, 2.2, and 3.3 nm), respectively.

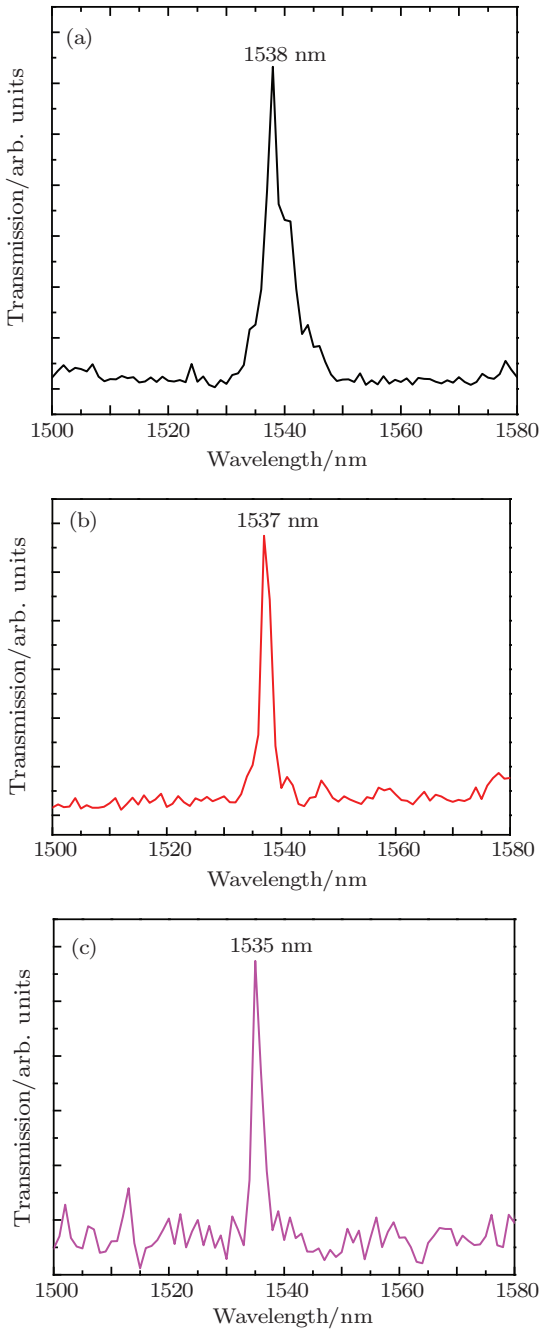


Fig. 6. (colour online) Measured transmission spectra of type-II filter by introducing cavities (a) C2, (b) C3, and (c) C4 to substitute cavity C1, respectively.

4. Conclusions

In summary, we have investigated both theoretically and experimentally the transmission properties of two-port resonant tunneling filters in 2D triangular lattice silicon PC slabs. In order to improve the filtering efficiency, a feedback method is introduced by closing the waveguide. Their optical properties were measured for different relative positions between closing waveguide boundary and resonator center, which is conducive to engender excellent filtering performance. Furthermore, the designed filters can feel the subtle change of the resonant cavities fabricated at present micro-fabrication precision, which is important to practical applications of the photonic devices in 2D PC slabs. This work reveals that the two-port resonant tunneling filter may be a promising element for future optical integrated circuits with ultra-compact dimension.

References

[1] Yablonovitch E 1987 *Phys. Rev. Lett.* **58** 2059

[2] John S 1987 *Phys. Rev. Lett.* **58** 2486

[3] Tokushima M and Yamada H 2002 *IEEE J. Quantum Electron.* **38** 753

[4] Han S Z, Tian J, Ren C, Xu X S, Li Z Y, Cheng B Y and Zhang D Z 2005 *Chin. Phys. Lett.* **22** 1934

[5] Tian J, Han S Z, Cheng B Y, Li Z Y, Feng S, Zhang D Z and Jin A Z 2005 *Acta Phys. Sin.* **54** 1218 (in Chinese)

[6] Tang H X, Zuo Y H, Yu J Z and Wang Q M 2008 *Chin. Phys.* B **17** 228

[7] Liu Y Z, Liu R J, Zhou C Z, Zhang D Z and Li Z Y 2008 *Opt. Express* **16** 21483

[8] Zhu Q Y, Fu Y Q, Hu D Q and Zhang Z M 2012 *Chin. Phys.* B **21** 064220

[9] Song B S, Noda S, Asano T and Akahane Y 2005 *Nature Mater.* **4** 207

[10] Akahane Y, Asano T, Song B S and Noda S 2005 *Opt. Express* **13** 1202

[11] Fan S, Villeneuve P R, Joannopoulos J D and Haus H A 1998 *Phys. Rev. Lett.* **80** 960

[12] Chutinan A, Mochizuki M, Imada M and Noda S 2001 *Appl. Phys. Lett.* **79** 2690

[13] Takano H, Akahane Y, Asano T and Noda S 2004 *Appl. Phys. Lett.* **84** 2226

[14] Takano H, Song B S, Asano T and Noda S 2005 *Appl. Phys. Lett.* **86** 241101

[15] Takano S, Song B S and Noda S 2006 *Opt. Express* **14** 3491

[16] Notomi M, Shinya A, Mitsugi S, Kuramochi E and Ryu H Y 2004 *Opt. Express* **2** 1551

[17] Shinya A, Mitsugi S, Kuramochi E and Notomi M 2005 *Opt. Express* **13** 4202

[18] Ren C, Tian J, Feng S, Tao H H, Liu Y Z, Ren K, Li Z Y, Cheng B Y, Zhang D Z and Yang H F 2006 *Opt. Express* **14** 10014

[19] Zhao Y N, Li K Z, Wang X H and Jin C J 2011 *Chin. Phys.* B **20** 074210

[20] Liu Y Z, Liu R J, Feng S, Ren C, Yang H F, Zhang D Z and Li Z Y 2008 *Appl. Phys. Lett.* **93** 241107

[21] Zhang Z Y and Qiu M 2006 *J. Opt. Soc. Am.* B **23** 104